

# Nonlinear Dynamics in Adaptive Echo Cancellation

William A. Sethares, Dept of Elec. and Comp. Eng.  
University of Wisconsin, Madison, WI 53706

Iven M. Mareels, Dept. of Elec. and Comp. Eng.  
University of Newcastle, Newcastle, NSW Australia

### Abstract

Adaptive hybrids are one way of cancelling the echo path in telephone systems. This paper illustrates a simplified model of an adaptive hybrid using two bifurcation parameters, the adaptive stepsize and the ratio of the two inputs. As these parameters vary, the system exhibits a wide variety of behaviors, including stable and unstable equilibrium points, stable and unstable periodic orbits, and aperiodic orbits. The underlying bifurcations include Hopf, flip, period doubling sequences, and a degenerate global bifurcation which gives rise to some very complex dynamics.

### Introduction

A device called a "4:2 hybrid" is used in telephone systems to transform the 4 wire long distance receive and transmit lines to and from a 2 wire local line. An ideal hybrid would move all the incoming signal from the 4 wire receive line to the 2 wire local line, and simultaneously move the outgoing signals from the 2 wire local line to the 4 wire transmit line. In a real device, however, some of the energy on the incoming line will inevitably leak into the outgoing line. One solution, called adaptive echo cancellation [1], [2], uses an adaptive filter to match the dynamics of the leakage path. See figure 1. When the near end speaker is silent, and when the adaptive filter has matched the transfer function of the hybrid, then  $\hat{y}$  will equal  $y$ , their difference is zero... and the echo of the far end speech is cancelled.

In certain situations, however, an intermittent "bursting" or "chirping" or "burping" misbehavior arises. This bursting cycle is characterized by a long drift phase, followed by large oscillations that quickly restabilize, returning again to the drift phase. To investigate the origin of this bursting, a simple model was introduced in [3] in which a single parameter ( $\hat{h}$ ) adaptive hybrid at the near end attempts to cancel the echo of the far end speech. At the far end, a (nonadaptive) hybrid is modeled as an attenuation  $\beta$  and a delay. Refer to figure 2, where  $\hat{v}_k/w_k$  represent the near/far end speech,  $h$  represents the echo path at the near end, and  $r_k/x_k$  represent the received/transmitted signals at the near end. Figure 3 shows a simulation of this model in which the transmit signal  $x_k$  is small, well behaved, and almost sinusoidal for over 4000 iterations. Suddenly, and without apparent warning,  $x_k$  oscillates rapidly and then settles down again. A second burst occurs at around 5800 iterations. Other bursts follow, on the average about 2000 iterations apart. Bursting was attributed to a lack of "persistent excitation" combined with the inherent feedback structure of the adaptive hybrid telephone system. It was conjectured that certain combinations of excitation might lead to chaotic behavior. This conjecture is examined in the

present paper, and numerous nonlinear behaviors are revealed, some of which may occur in physically reasonable situations. The bursting is revealed to be either a region of stable aperiodic orbits, a marginally stable two periodic orbit or (perhaps) a strange attractor, depending on the relative magnitudes of the two inputs to the system, and depending on the adaptive stepsize parameter.

The system model, from [3], is

$$\hat{h}_{k+1} = \hat{h}_k - \mu' x_k^2 \hat{h}_k - \mu' x_k \hat{v}_{k+1}, \quad (1.1)$$

where  $\hat{h}_k = h - \hat{h}_k$  and the transmit signal  $x_k$  is

$$x_{k+1} = w_{k+1} + \beta r_{k+1} \\ = \beta \hat{h}_k x_k + \beta \hat{v}_{k+1} + w_{k+1}. \quad (1.2)$$

The equation pair (1.1) and (1.2) is a two state ( $\hat{h}_k, x_k$ ) nonlinear equation with two inputs,  $\hat{v}_k$  and  $w_k$ . With  $v_k = \beta \hat{v}_k$  and  $h_k = \beta \hat{h}_k$ , this is equivalent to the mapping  $F: \mathbb{R}^2 \rightarrow \mathbb{R}^2$ ,

$$F \begin{pmatrix} y \\ h \end{pmatrix} = \begin{pmatrix} h y + v + w \\ h - \mu y^2 h - \mu v y \end{pmatrix} \quad (1.3)$$

The simplest case of (1.3) is a "D.C." or steady state analysis in which the inputs are held constant. Reparametrize (1.1) - (1.2) with  $v_k = v$  and  $w_k = w$  for every  $k$ . Let  $\mu = \mu'/w^2$ ,  $\alpha = \beta v/w$ ,  $h_k = \beta \hat{h}_k$ , and  $y_k = x_k/w$ . The system is then

$$F \begin{pmatrix} y \\ h \end{pmatrix} = \begin{pmatrix} h y + \alpha + 1 \\ h - \mu y^2 h - \mu \alpha y \end{pmatrix} \quad (1.4)$$

In (1.4),  $h$  and  $y$  represent the states of the system ( $h$  is the loop gain,  $y$  is the received signal), while  $\mu$  and  $\alpha$  are the bifurcation parameters. Physically,  $\mu$  represents a scaled version of the stepsize of the adaptive algorithm, while  $\alpha$  is proportional to the *ratio* of the power of the two constant inputs  $v$  and  $w$ . Since  $\mu'$  of (1.1) is a parameter chosen by the system designer, and since

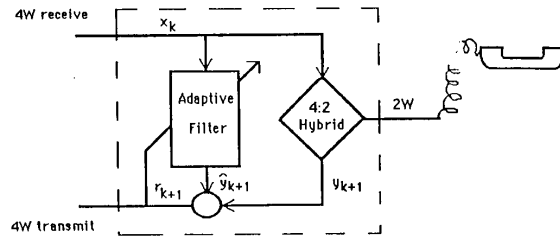


Figure 1: Basic adaptive hybrid

an upper bound on  $v$  and  $w$  are dictated by the physical properties of the telephone system (size of wires, maximum voltage swings, etc.), the case of most physical interest is when  $\mu$  is "small." The large  $\mu$  case exhibits regions of period doubling leading to

chaos much as the large stepsize adaptive regulator of [4] leads to such behavior.

The parameter  $\alpha$ , however, has no such natural limitations on magnitude, since the ratio  $\beta v/w$  can

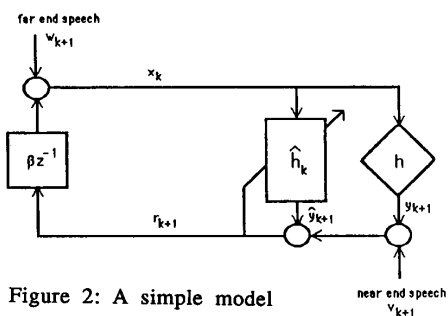


Figure 2: A simple model

reasonably assume any real value, with small  $w$  corresponding to large  $\alpha$ . Speaking imprecisely (but nonetheless reasonably), small  $\alpha$  correspond to a high degree of persistence of excitation of the adaptive algorithm, while large  $\alpha$  correspond to a low degree of excitation. It is, of course, the latter which exhibit the more exotic (mis)behaviors. Since the excitation levels cannot generally be manipulated by the system designer, such exotic behaviors cannot be ruled out in applications.

The body of the paper presents numerous simulations which examine the behavior of the hybrid system (1.4) for various values of stepsize  $\mu$  and excitation  $\alpha$ . The pictures show equilibrium points, two periodic orbits, and aperiodic orbits. Sometimes several orbits coexist on the same phase plane. As the parameter  $\alpha$  unfolds, several types of bifurcations are apparent, including Hopf, flip, and a family of degenerate global bifurcations. For large values of the bifurcation parameter, unwanted instabilities due to a "large stepsize" are encountered.

While many of these behaviors (and our observations about those behaviors) can be proven [5], the last few pictures go beyond tractability. When the inputs are sinusoidal, all the bizarre behaviors are found, and some new phenomena are revealed. The final section presents our conclusions: the bursting phenomena is one of three behaviors depending on the conditions under which the system operates, bursting is inherent in underexcited adaptive systems which are encased in a feedback loop, and persistence of excitation is virtually necessary for the good performance of such adaptive systems.

#### Picture Gallery

The simplest version of (1.4) is when the adaptation is frozen with a zero stepsize. Though physically uninteresting, this case already exhibits some nontrivial behaviors. With  $\mu=0$ , (1.4) becomes

$$F \begin{pmatrix} y \\ h \end{pmatrix} = \begin{pmatrix} h y + \alpha + 1 \\ h \end{pmatrix} \quad (2.1)$$

which has equilibria at  $y^* = \frac{\alpha+1}{1-h^*}$  and  $h^*$  arbitrary ( $h^* \neq 1$ ). This equilibrium is stable when  $|h^*| < 1$  (though

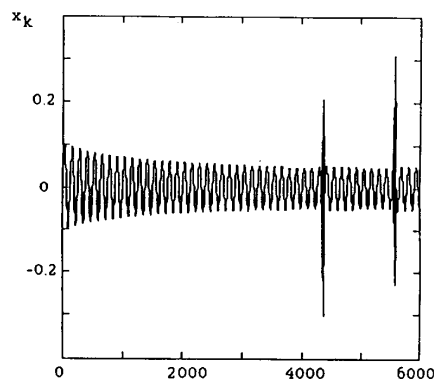


Figure 3: Bursting in hybrid model.

not asymptotically stable in the  $h$  direction) while it is unstable for  $|h^*| > 1$ . When  $h^* = 1$ , the map is a pure integrator and hence is unstable (except for the singular point  $\alpha = -1$ ). At  $h^* = -1$ , (2.1) is again stable (though not asymptotically in either  $h$  or  $y$ ).

For  $h^* = -1$  there is also a family of stable 2 periodic orbits, since  $y_{k+2} = y_k$ . This information on the behavior of (2.1) is presented graphically in figure 4. Clearly, when  $h$  is allowed to vary by considering nonzero  $\mu$ , the behavior of the system will be at least this complicated, involving both equilibria and periodic orbits.

When  $\mu \neq 0$ ,  $F$  has a unique fixed point at  $y^* = 1$ ,  $h^* = -\alpha$ . For  $\alpha = -1$ , there is an isolated fixed point at  $y^* = 1$ ,  $h^* = 1$ , and a subspace of fixed points at  $y^* = 0$ ,  $h^*$  arbitrary. The stability of the isolated fixed points can be addressed by examining the eigenvalues of the Jacobian of  $F$  evaluated at  $y^*$ ,  $h^*$ . Writing out  $DF(y^*, h^*)$  and applying the Jury test for stability shows that the eigenvalues of  $DF$  are less than unity if and only if  $\alpha > -1$ ,  $\mu > 0$ , and  $\alpha < 1 - \mu/2$  are satisfied simultaneously. This region is shaded in figure 5. All points on the boundary of this region are bifurcation points, since they represent values of  $\alpha$  and/or  $\mu$  for which the magnitude of the eigenvalues of  $DF$  are exactly unity.

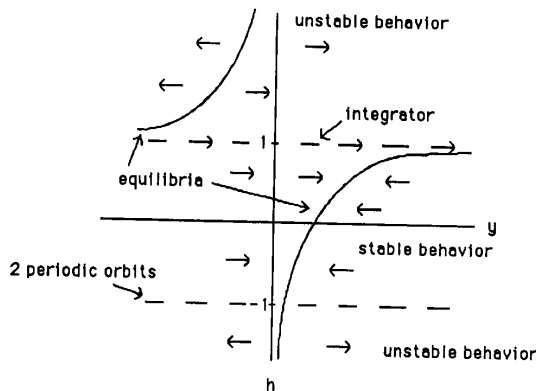


Figure 4: Phase portrait for  $\mu=0$

For  $\mu < 0$  and  $\mu > 4$  there are no critical points and the system (1.4) is always unstable. These have simple physical explanations. Negative  $\mu$  corresponds

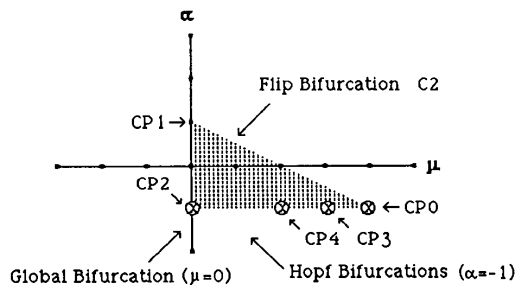


Figure 5: Bifurcation diagram  $\alpha$  vs.  $\mu$

to a reversal of the sign of the adaptation gain, while  $\mu > 4$  corresponds to instability induced by violation of the 'small stepsize' requirement. The parameter error in these cases diverges at an exponential rate, and simulations are typically arrested by numerical overflow within several dozen iterations.

When  $0 < \mu < 4$ , there are two critical points. For  $\alpha = 1 - \mu/2$ , one eigenvalue is at  $-1$ , indicating that these are *flip* bifurcations which shed a two periodic orbit as  $C2$  is crossed. Inside the triangle, simulations are very boring - both states rapidly converge to the equilibrium. As the  $C2$  line is crossed, the equilibrium bifurcates into a two period orbit.

The dynamics near the  $\alpha = -1$  line are more involved. These are Hopf bifurcations with both eigenvalues on the unit circle for  $0 < \mu < 4$ . Figure 6 shows an aperiodic orbit for  $\alpha = -1.05$ . Inside the two circles is an unstable 2 periodic orbit. The trajectory bounces from circle to circle at each iteration, and 'fills in' the perimeter of the circles without ever returning to exactly the same values. As  $\mu$  varies from 0 to 4, the roots move around the unit circle through the whole spectrum of possible Hopf bifurcations. Degeneracies occur at  $\mu = 0$  (CP2 of figure 5 with double 1 eigenvalue), at  $\mu = 2$  (CP4 with eigenvalues  $\pm i$ ), at  $\mu = 3$  (CP3 with eigenvalues at  $-0.5 \pm i\sqrt{3}/2$ ), and at  $\mu = 4$  (CP0 with a double eigenvalue at  $-1$ ).

For the global bifurcation point  $\alpha = -1$ , the eigenvalues of  $DF$  are at 1 and  $h^*$  for any  $h^*$ , and the subspace  $y^* = 0$  is attractive for  $|h^*| < 1$ , and repellant for  $|h^*| > 1$ . Figure 7 gives a graphic interpretation of the behavior of the phase trajectories of the system. In the left half plane, the trajectories bounce from top to bottom at alternate iterations, eventually flowing into one of the attractive points at  $y^* = 0$  and  $|h^*| < 1$ . In the right half plane, trajectories move straight to the  $y^* = 0$  line or they become trapped about the equilibrium at  $(1, 1)$ . The  $h = -1$  point is the germ that starts the two periodic orbit that later undergoes a Hopf bifurcation. The  $h = 1, y = 1$  point is the fixed point analyzed above which undergoes a Hopf bifurcation and is the origin of the stable aperiodic orbits of figure 6 seen for  $\alpha$  near  $-1$ .

As  $\alpha$  crosses the  $-1$  bifurcation point, several things happen. Compare figure 7 with figure 8, which shows a phase portrait of several trajectories for  $\alpha = -1.02$ . First, the equilibrium and the surrounding orbits become unstable. This is pictured in the outward spiral in the upper right hand corner of figure 8. (The arrows have been added to the simulation to indicate the general direction of motion.) Second, the  $y = 0, h = -1$  point splits into an unstable two periodic orbit. These are the small  $x$ 's inside the small circles near the  $h = -1$  point. Most likely, the circles themselves are stable aperiodic orbits. Third, the subspace of equilibria disappears, and is replaced by a long, slowly moving trajectory that channels the right half plane trajectories to the aperiodic orbit near  $h = -1$ . This is the "linear" drift phase in which the parameter error slowly accumulates.

There is a stable equilibrium only for values of  $\alpha$  within the triangular region of figure 5. When there is a no stable fixed point, the next simplest possible behavior is that there might be low period orbits. The flip bifurcation indicates the existence of two-periodic orbits for systems whose parameters are above (but close to) the  $C2$  line. Two-periodic orbits can be investigated by finding the equilibria of  $F^2:R^2 \rightarrow R^2$  which can be calculated directly from (1.3). Details are in [5].

Since  $\mu = 0, h = -1$  gives rise to a two-periodic orbit, it is not surprising that some of these orbits persist for nonzero  $\mu$ . In fact, there are equilibria of  $F^2$  at  $h = -1 + O(\mu)$ . For example, setting  $\alpha = 1.2$  and  $\mu = 0.01$ , and calculating 50,000 iterations of (1.3) leads to the two periodic solution  $(-0.9962, 1.4395)$  and  $(-0.9928, 0.7660)$ . This is clearly a stable 2 periodic orbit. In contrast, set  $\alpha = -1.05$  without changing  $\mu$ . The simulation does not settle into a two periodic orbit even after 25 million iterations! See figure 6.

The stability of a two period map can be determined by the eigenvalues of the Jacobian of the two iteration map, that is, the eigenvalues of

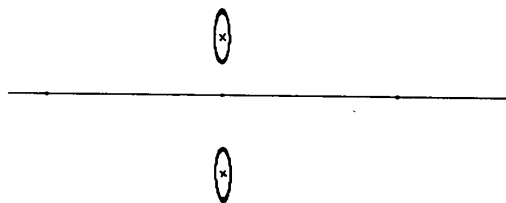


Figure 6: Aperiodic orbits at  $\alpha = -1.05$

$DF^2(y^*, h^*)$ . The first example is within the stability region for the two periodic orbit, and hence it converges to this orbit. This illustrates the effect of the flip bifurcation at  $\alpha = 1 - \mu/2$  in which the stable equilibrium for  $0 < \alpha < 1 - \mu/2$  is transformed into a stable two periodic orbit when  $\alpha > 1$ . The second example is in the region where 2 periodic orbits are unstable and the system does not converge to a 2 period solution. The two points of the unstable 2 periodic orbit are the  $x$ 's inside the circles of figure 6.

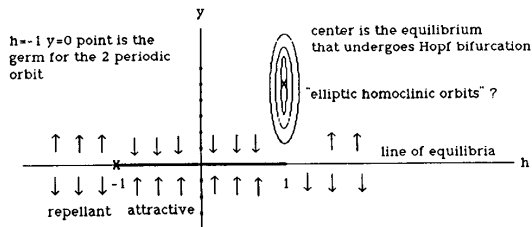


Figure 7: Global bifurcation point  $\alpha=-1$

As  $\alpha$  decreases further (a small amount that appears to go to zero as the stepsize  $\mu$  vanishes), the aperiodic orbits grow larger, until at  $\alpha \sim 1.04$  (for  $\mu = .01$ ) they touch. At this point, another qualitative change occurs - the aperiodic orbits become unstable, and the behavior of figure 9 appears. Again, the unstable 2 period orbit is marked by the small x's in the center, and the trajectories jump from oval to oval at alternate iterations. They never seem to settle down to nice smooth curves... this simulation was begun after 25 million iterations... one can only suppose that the tattered edges of this figure are not transients that will die away, but rather are an intrinsic feature of its behavior.

How large can  $\alpha$  get and still retain stability of this two periodic orbit? An approximate analysis gives  $\alpha \sim 7$  as an upper bound for stability and simulations show a bifurcation point at  $\alpha = 6.4$ , when a four periodic orbit comes into existence. This is the beginning of a period doubling sequence leading into chaos, as suggested by the simulations in figure 10. Physically, this can be interpreted as a violation of the "small stepsize" assumption. Note that as  $\mu$  is decreased, the two periodic sequence remains stable for larger and larger  $\alpha$ . These instabilities eventually overwhelm the system, and we lose the ability to track the behavior for larger  $\alpha$ .

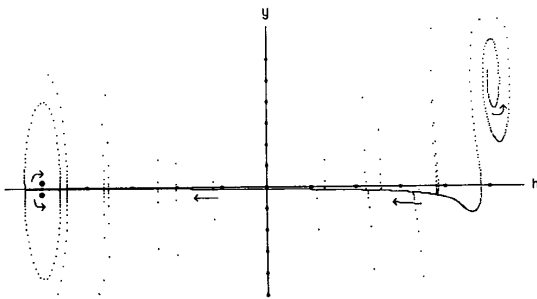


Figure 8: Phase portrait for  $\alpha=-1.2$

### Conclusions

We have three possible explanations of the observed bursting behavior of the adaptive hybrid. For  $\alpha > 1$ , the bursting may be a transient phenomena that will eventually decay into a two periodic orbit. For  $\alpha$  near  $-1$ , the bursting may be an aperiodic orbit. For  $\alpha \ll -1$ , the bursting may be due to some yet unclassified dynamics (as in figure 9)

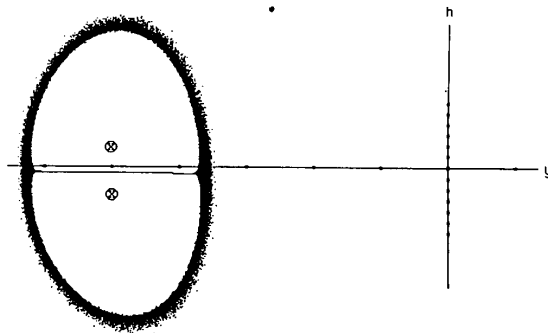


Figure 9: Phase portrait  $\alpha=-1.2$   
(begun after 25,000,000 iterations)

due to the degenerate Hopf bifurcation. In the latter two cases, the behavior is not transient and will not die away with time.

In surveying the adaptive literature, there have been numerous attempts to both describe and explain the misbehaviors of adaptive systems. It appears that virtually all adaptive systems which incorporate the adaptive element inside a feedback loop (the hybrid, IIR identification, adaptive control, etc.) are susceptible to the same range of possible misbehaviors due to underexcitation as the present system. In essence, this suggests that the persistence of excitation conditions are virtually necessary to assure that one remains in the "good" operating region.

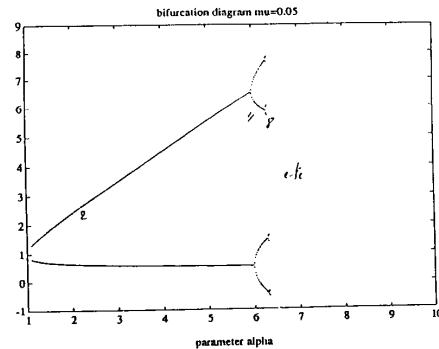


Figure 10: Period doubling

### References

- [1] M. L. Honig and D. G. Messerschmitt, *Adaptive Filters: Structures, Algorithms, and Applications*, Kluwer Academic, 1984.
- [2] B. Widrow and S. D. Stearns, *Adaptive Signal Processing*, Prentice-Hall, 1985.
- [3] W. A. Sethares, C. R. Johnson Jr. and C. Rohrs, "Bursting in adaptive hybrids," *IEEE Trans. on Communications*, Aug 1989.
- [4] I. M. Y. Mareels and R. R. Bitmead, "Non-linear dynamics in adaptive control: chaotic and periodic stabilization," *Automatica*, vol. 22, no. 6, 1985.
- [5] W. A. Sethares, I. M. Y. Mareels and L. Praly, "Dynamics of the adaptive hybrid," submitted to *IEEE Trans. on Circuits and Systems*.